Design and Comprehensive Conformational Studies of Tyr^1-cyclo(D-Pen^2-Gly^3-Phe^4-L-3-Mpt^5) and Tyr^1-cyclo(D-Pen^2-Gly^3-Phe^4-D-3-Mpt^5): Novel Conformationally Constrained Opioid Peptides

Gregory V. Nikiforovich,*,† Katalin E. Kövér,‡ Stephen A. Kolodziej,§ Bruce Nock,⊥ Clifford George,∥ Jeffrey R. Deschamps,∥ Judith L. Flippen-Anderson,∥ and Garland R. Marshall†,§

Contribution from the Center for Molecular Design and Departments of Pharmacology and Psychiatry, Washington University, St. Louis, Missouri 63130, L. Kossuth University, H-4010 Debrecen, Hungary, and Laboratory for the Structure of Matter, Naval Research Laboratory, Washington, DC 20375

Received August 28, 1995⊗

Abstract: Two compounds, Tyr^1-cyclo(D-Pen^2-Gly^3-Phe^4-L-3-Mpt^5) (DPMPT; 3-Mpt is *trans*-3-mercaptoproline) and Tyr^1-cyclo(D-Pen^2-Gly^3-Phe^4-D-3-Mpt^5) (DPDMPT), were designed employing energy calculations. Geometrical comparison showed that some low-energy 3D structures of DPMPT and DPDMPT are compatible with the model for the δ-receptor-bound conformation of the well-known δ-selective DPDPE peptide Tyr^1-cyclo(D-Pen^2-Gly^3-Phe^4-D-Pen^5, which was proposed by us earlier. DPMPT and DPDMPT were tested for their binding to δ-, μ- and κ-opioid receptors. The corresponding K_i values were 3.5, 68, and >5000 nM for DPMPT, and 103.7, >5000, and >5000 nM for DPDMPT, respectively. Independent studies by homo- and heteronuclear NMR spectroscopy and energy calculations showed that DPMPT exists in DMSO solution in conformational equilibrium among several backbone conformations with the same type of 3D structure for the cyclic moiety, but with somewhat different conformers of the acyclic part of the molecule and two types of rotamers for the D-Pen side chain, namely, **t** and $\mathbf{g}^-$. For DPDMPT, energy calculations combined with the NMR data suggest that any one out of four low-energy conformers belonging to the same type of the backbone of the cyclic moiety may be a possible candidate for the DPDMPT conformer in DMSO. The DPDMPT structure revealed by X-ray crystallography showed remarkable similarity to DPDMPT solution conformations. The determined solution conformations of both compounds were compared to their suggested δ-receptor-bound conformers. Results of comparison showed that all four of the possible solution conformations of DPDMPT are nonsimilar to the DPDMPT δ-receptor-bound conformation, whereas two of the possible solution conformations of DPMPT are compatible with the suggested δ-receptor-bound conformation of DPMPT. This finding can explain the difference in binding of DPMPT and DPDMPT to δ-opioid receptors by a suggestion that the δ-receptor-bound conformation of DPMPT already preexists in solution, whereas solution conformations of DPDMPT should be more significantly distorted to match the δ-receptor-bound conformation of DPDMPT.

Introduction

The search for nontraditional opioid analgesics that do not interact with μ-receptors to avoid dependence is current in modern molecular pharmacology (see, e.g., refs 1 and 2). A number of advantages are expected from opioids, which can act *via* δ-opioid receptors. Among these advantages are production of analgesia with decreased development of physical dependence, lack of depression of respiratory function, lack of adverse gastrointestinal effects, *etc*.

Various researchers have presented their models of δ-receptor pharmacophores during the last several years. There were mostly studies of highly δ-selective peptides, such as DPDPE [Tyr^1-cyclo(D-Pen^2-Gly^3-Phe^4-D-Pen^5)], using NMR spectroscopy,[3,4] X-ray crystallography, and a variety of theoretical methods.[5−14] We have also developed a model for δ-receptor pharmacophores on the basis of energy calculations and subsequent geometrical comparison of low-energy conformers

* To whom correspondence should be addressed.
† Center for Molecular Design, Washington University.
‡ L. Kossuth University.
§ Department of Pharmacology, Washington University.
⊥ Department of Psychiatry, Washington University.
∥ Naval Research Laboratory.
⊗ Abstract published in *Advance ACS Abstracts,* January 15, 1996.

(1) Cheng, P. Y.; Wu, D. L.; Decena, J.; Cheng, Y.; McCabe, S.; Szeto, H. H. *J. Pharmacol. Exp. Ther.* **1992**, *262*, 1004−1010.
(2) Portoghese, P. S. *J. Med. Chem.* **1991**, *34*, 1757−1762.
(3) Hruby, V. J.; Kao, L.-F.; Pettitt, B. M.; Karplus, M. *J. Am. Chem. Soc.* **1988**, *110*, 3351−3359.
(4) Mosberg, H. I.; Sobczyk-Koiro, K.; Subramanian, P.; Crippen, G.; Ramalingam, K.; Woodard, R. W. *J. Am. Chem. Soc.* **1990**, *112*, 822−829.
(5) Keys, C.; Payne, P.; Amsterdam, P.; Toll, L.; Loew, G. *Mol. Pharmacol.* **1988**, *33*, 528−536.
(6) Nikiforovich, G. V.; Balodis, J.; Shenderovich, M. D.; Golbraikh, A. A. *Int. J. Pept. Protein Res.* **1990**, *36*, 67−78.
(7) Froimowitz, M.; Hruby, V. J. *Int. J. Pept. Protein Res.* **1989**, *34*, 88−96.
(8) Froimowitz, M. *Biopolymers* **1990**, *30*, 1011−1025.
(9) Chew, C.; Villar, H. O.; Loew, G. H. *Mol. Pharmacol.* **1991**, *39*, 502−510.
(10) Wilkes, B. C.; Schiller, P. W. *J. Comput.-Aided Mol. Des.* **1991**, *5*, 293−302.
(11) Pettitt, B. M.; Matsunaga, T.; Al-Obeidi, F.; Gehrig, C.; Hruby, V. J.; Karplus, M. *Biophys. J.* **1991**, *60*, 1540−1544.
(12) Smith, P. E.; Dang, L. X.; Pettitt, B. M. *J. Am. Chem. Soc.* **1991**, *113*, 67−73.
(13) Chew, C.; Villar, H. O.; Loew, G. H. *Biopolymers* **1993**, *33*, 647−657.
(14) Flippen-Anderson, J. L.; Hruby, V. J.; Collins, N.; George, C.; Cudney, B. *J. Am. Chem. Soc.* **1994**, *116*, 7523−7531.

0002-7863/96/1518-0959$12.00/0

of DPDPE and other cyclic and linear peptides, which possess good δ-receptor preference and compete with DPDPE for the same receptor site, JOM-13 (Tyr[1]-cyclo(D-Cys[2]-Phe[3]-D-Pen[4]) and dermenkephalin (DRE, Tyr[1]-D-Met[2]-Phe[3]-His[4]-Leu[5]-Met[6]-Asp[7]-NH_2).[15]

A model of the receptor-bound conformer for δ-opioid peptides should take into account the similarity in the mutual spatial arrangement of the N-terminal α-amino group and the side chains of the Tyr[1] and Phe[4(3)] residues. On the basis of comparison, one particular structure was found to be geometrically similar for all δ-selective compounds (DPDPE, JOM-13, and DRE), defining a prototype model for the δ-receptor-bound conformation. The most characteristic feature of the model was the placement of the Phe side chain in a more or less definite position in the space corresponding to a χ_1 rotamer that is $\mathbf{g}^-$ for peptides containing Phe[4] and **t** for peptides with Phe[3]. The position in space for the Tyr[1] side chain was not specified as precisely.[11,15,16]

The proposed model was strongly supported by synthesis and biological testing of conformationally constrained analogs of deltorphin I, a δ-selective linear peptide (Tyr-D-Ala-Phe-Asp/Glu-Val-Val-Gly-NH_2, DT I/II).[16,17] Energy calculations for the [D-Cys[2],Cys[5]]-DT I analog found low-energy conformers, which were very similar to the model of the δ-receptor-bound conformer. On the basis of these calculations, several cyclic analogs of DT I were synthesized and tested for their receptor binding and biological potency. Results showed that [D-Cys[2],-Cys[5]]-DT I was as active as linear DT I at δ-receptors, but much more active at μ-receptors; in the similar [D-Cys[2],Pen[5]]-DT I cyclic analog, the δ-selectivity was restored.

Another confirmation of the proposed model came from the synthesis of a conformationally restricted analog of the μ-selective dermorphin peptide (DRM).[18,19] Our model requires the side chain of the Phe[3] residue to possess a **t** rotamer to enhance the δ-selectivity of an analog. Tourwé et al.[18,19] have fixed the Phe[3] side chain of DRM into this conformation by bridging the phenyl ring and the nitrogen atom of the succeeding amino acid by a methylene group. It excludes the $\mathbf{g}^-$ rotamer of the Phe[3] side chain, but allows **t** and $\mathbf{g}^+$ rotamers. This modification alone has shifted the selectivity profile for this DRM analog from μ- to δ-selectivity. This trend was observed recently by the same group with other conformationally restricted opioid peptides.[20] On the other hand, [Tic[3]]-DRM, where the Phe side chain was fixed into the $\mathbf{g}^+$ rotamer (Tic is a tetrahydroisoquinoline-3-carboxylic acid), was inactive on both receptor types.[19] Interestingly, the $\mathbf{g}^-$ rotamer for the Phe[3] side chain was observed in the X-ray studies of JOM-13.[21]

The importance of the $\mathbf{g}^-$ rotamer for the Phe[4] side chain in the δ-receptor-bound conformer for opioid peptides was confirmed also by the results of energy calculations for β-Me-Phe[4]-substituted analogs of DPDPE.[11,15] It appeared that a strong preference of the β-Me-Phe[4] side chain for rotamer $\mathbf{g}^-$ was found for (*S*,*S*)-β-Me-Phe-DPDPE, **t** for (*S*,*R*)- and (*R*,*S*)-β-Me-Phe-DPDPE, and $\mathbf{g}^+$ for (*R*,*R*)-β-Me-Phe-DPDPE. The (*S*,*S*)-β-Me-Phe-DPDPE analog was the most potent out of the four at the δ-receptors.[22] Finally, a recent paper on the X-ray structures of DPDPE[14] delivered further evidence confirming our model. It was clearly stated in the paper that our model for the δ-receptor-bound conformer matches one of the DPDPE conformers revealed by X-ray studies in spatial arrangement of functionally important side chains.[14]

The main goal of the present study was to use this model as a template for the computational design of novel rigidified analogs of DPDPE with high potency of binding and δ-selectivity employing "chimeric" mercaptoproline amino acids. Such analogs were prepared and subjected to comprehensive conformational studies, including energy calculations, NMR spectroscopy, and X-ray crystallography. All these methods have been employed independently to produce highly consistent results, providing strong structural support for the 3D model in question. Such novel analogs might be used, in turn, as promising leads for δ-selective peptidomimetics.

Results

Design of DPMPT Peptides by Energy Calculations. The systematic use of chimeric amino acids as conformational constraints in peptides has been suggested previously.[23] Some, like α-methylamino acids, are used to stabilize right or left α-helical conformers of the peptide backbone for this particular residue. Others are used for intramolecular cyclization. In this respect, mercaptoprolines are of special importance. Mercaptoprolines limit conformational freedom of the peptide backbone by restricting its own ϕ dihedral angle, as well as the ψ angle for the preceding residue.[23] At the same time, they could be used for intramolecular cyclization by forming disulfide bridges with other residues with side chains bearing sulfhydryl groups. We were very successful in incorporating *trans*-4-mercaptoprolines in the angiotensin (AT) sequence to obtain analogs cyclo[Sar[1],Hcy[3],4-Mpt[5]]-AT and cyclo[Sar[1],Cys[3],4-Mpt[5]]-AT, which showed excellent AT_1 and AT_2 receptor binding.[24] NMR data were indicative of well-defined solution conformations for the cyclic moieties of these analogs, which made possible some conclusions on the model of AT receptor-bound conformation.[25]

It, therefore, seemed logical to replace the D-Pen[5] residue of DPDPE by *trans*-3-mercaptoproline (3-Mpt) both in L- and D-configurations, since DPLPE, the analog featuring the L-Pen[5] residue instead of the D-Pen[5] residue, was known to be almost as δ-selective as DPDPE itself. Accordingly, energy calculations were performed for the two analogs Tyr[1]-cyclo(D-Pen[2]-Gly[3]-Phe[4]-L-3-Mpt[5] (DPMPT) and Tyr[1]-cyclo(D-Pen[2]-Gly[3]-Phe[4]-D-3-Mpt[5] (DPDMPT) as described in the Experimental Section. The calculations included the search for all low-energy conformers of peptide backbones of both analogs, as well as the search for energetically optimal rotamers of side chains for the Tyr, D-Pen, and Phe residues. Finally, 49 low-energy

(15) Nikiforovich, G. V.; Hruby, V. J.; Prakash, O.; Gehrig, C. A. *Biopolymers* **1991**, *31*, 941−955.
(16) Misicka, A.; Nikiforovich, G. V.; Lipkowski, A. W.; Horvath, R.; Davis, P.; Kramer, T. H.; Yamamura, H. I.; Hruby, V. J. *Bioorg. Med. Chem. Lett.* **1992**, *2*, 547−552.
(17) Misicka, A.; Lipkowski, A. W.; Horvath, R.; Davis, P.; Kramer, T. H.; Yamamura, H. I.; Porecca, F.; Hruby, V. J. In *Peptides − 1992. Proceedings of the 22nd European Peptide Symposium*; Schneider, C., Ed.; ESCOM: Leiden, 1992; pp 651−652.
(18) Tourwé, D.; Verschueren, K.; Van Binst, G.; Davis, P.; Porecca, F.; Hruby, V. J. *Bioorg. Med. Chem. Lett.* **1992**, *2*, 1305−1308.
(19) Tourwé, D.; Toth, G.; Lebl, M.; Verschueren, K.; Knapp, R. J.; Davis, P.; Van Binst, G.; Yamamura, H. I.; Burks, T. F.; Kramer, T.; Hruby, V. J. In *Peptides. Chemistry and Biology. Proceedings of the Twelfth American Peptide Symposium*; Smith, J. A., Rivier, J. E., Eds.; ESCOM: Leiden, 1992; pp 307−308.
(20) Tourwé, D.; Conrath, P.; Frycia, A.; Verschueren, K.; Jaspers, H.; Verheyden, P.; Van Betsbrugge, J.; Van Binst, G. In *Peptides 1994. Proceedings of the Twenty-Third European Peptide Symposium*; Maia, H. L. S., Ed.; ESCOM: Leiden, 1995; pp 700−701.
(21) Lomize, A. L.; Flippen-Anderson, J. L.; George, C.; Mosberg, H. I. *J. Am. Chem. Soc.* **1994**, *116*, 429−436.
(22) Hruby, V. J.; Toth, G.; Gehrig, C. A.; Kao, L.-F.; Knapp, R.; Lui, G. K.; Yamamura, H. I.; Kramer, T. H.; Davis, P.; Burks, T. F. *J. Med. Chem.* **1991**, *34*, 1823−1830.
(23) Marshall, G. R. *Tetrahedron* **1993**, *49*, 3547−3558.
(24) Plucinska, K.; Kataoka, T.; Yodo, M.; Cody, W. L.; He, J. X.; Humblet, C.; Lu, G. H.; Lunney, E.; Major, T. C.; Panek, R. L.; Schelkun, P.; Skeean, R.; Marshall, G. R. *J. Med. Chem.* **1993**, *36*, 1902−1913.
(25) Nikiforovich, G. V.; Kao, J. L.-F.; Plucinska, K.; Zhang, W. J.; Marshall, G. R. *Biochemistry* **1994**, *33*, 3591−3598.

Table 1. Low-Energy Conformers of DPMPT and DPDMPT Compatible with Model for the δ-Receptor-Bound Conformation of DPDPE (see Table VII in Ref 15)

	Tyr		D-Pen[2]		Gly		Phe			3-Mpt/D-Pen[5]	
	ψ	χ_1	ϕ	ψ	ϕ	ψ	ϕ	ψ	χ_1	ω	ϕ
DPMPT	141	180	79	21	−86	−25	−140	73	−60	167	−75
DPDMPT	140	180	78	35	−94	−33	−141	73	−60	15	75
	145	60	78	36	−95	−34	−140	73	−61	16	75
DPDPE	142	−180	80	−145	66	27	−157	−57	−75	179	126

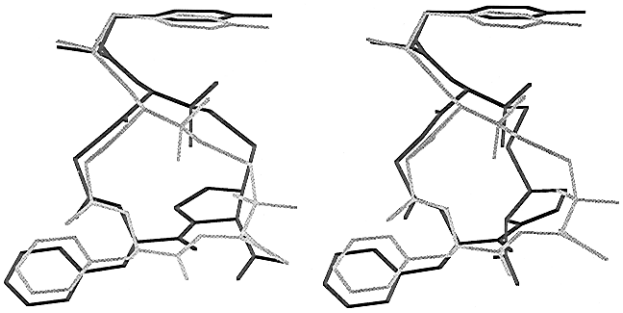

Figure 1. Suggested δ-receptor-bound conformers for DPMPT (left) and DPDMPT (right), both in bold, overlapped with the δ-receptor-bound conformer for DPDPE proposed earlier (lighter lines). All hydrogens are omitted.

conformers ($E - E_{min} \leq 5$ kcal/mol) differing by conformations of backbone and by rotamers of the mentioned residues were found for DPMPT, and 85 for DPDMPT. (These numbers correspond to calculations performed with $\epsilon = 2.0$, which is a standard value for the ECEPP force field; see the Experimental Section.) The most interesting common feature of all low-energy conformers for both analogs is that they are drastically different as to the conformation of the peptide bond preceding the mercaptoprolines. Namely, all conformers of DPMPT possess the *trans*-conformation of the L-3-Mpt residue, whereas all conformers of DPDMPT possess the *cis*-conformation of the D-3-Mpt residue.

Each low-energy conformer of DPMPT and DPDMPT was compared with the proposed models for the δ-receptor-bound conformation of DPDPE[15] by overlapping the atomic centers, which were used initially for deducing the model itself, namely, the nitrogen atom of the α-amino group, the C^{γ} and C^{ζ} atoms of the Tyr and the Phe aromatic rings, and the C^{α} atom of the D-Pen residue. Comparison was performed by RMS calculations for those six atoms with the additional requirement that any of the six individual distances between the same atomic centers in the compared pair of conformers should be less than 1 Å. Results of comparison showed that only one of the 3D structures of DPMPT is compatible with one model for the δ-receptor-bound conformation of DPDPE (RMS 0.53 Å, **t** rotamer of the Tyr side chain), and two of the 3D structures of DPDMPT are compatible with two of the models for the δ-receptor-bound conformation of DPDPE (RMS 0.57 Å, **t** rotamer of the Tyr side chain, and RMS 0.64 Å, $\mathbf{g}^+$ rotamer of the Tyr side chain). The values of dihedral angles for those structures are listed in Table 1, and their overlaps with the model for the δ-receptor-bound conformation of DPDPE (**t** rotamer of the Tyr side chain) are depicted in Figure 1.

It is obvious from Figure 1 that both DPMPT and DPDMPT possess good compatibility with the model for the δ-receptor-bound conformation of DPDPE as to the spatial arrangement of the N-terminal α-amino group and the side chains of the Tyr and Phe residues. It might be noteworthy that this compatibility occurs despite differences in the dihedral angle values of the backbone for comparable conformers (see Table 1). This compatibility suggests that both DPMPT and DPDMPT should show high potency in binding to δ-opioid receptors, provided that no functional group other than those mentioned influences the binding. At the same time, the spatial location of bulky substituents of the C^{β} atom of the residue in position 5, which may be important for δ-vs μ-selectivity (see, e.g., ref 26), is closer for DPMPT and DPDPE than for DPDMPT and DPDPE (Figure 1).

Table 2. Results of Binding Assays for Different Types of Opioid Receptors

	K_i (nM)		
compound	δ	μ	κ
DPDPE	1.7	576	>4000
DPMPT	3.5	68	>5000
DPDMPT	103.7	>5000	>5000

Synthesis. Synthesis of the cyclic pentapeptides followed our previously published methodology for synthesis of the CCK/opioid analogs containing 3-Mpt.[27] Linear peptides were assembled via standard solid phase peptide synthesis, and two diastereomeric peptides resulted from the use of racemic 3-Mpt. The diastereomers were separated by preparative reversed phase HPLC prior to cyclization using potassium ferricyanide as the oxidant. Yields of the cyclizations were approximately 25% for the monomers; considerable amounts of symmetric and asymmetric dimers were formed as byproducts. No efforts were made to optimize the cyclizations for this study. It was also noted that prolonged hydrolyses were required in order to obtain adequate results from the amino acid analyses, as we previously reported for the CCK/opioid chimeric peptides.[27]

Biological Testing. DPMPT and DPDMPT were tested for their binding to three types of opioid receptors, namely, μ-, δ-, and κ- (see the details in the Experimental Section). The results are listed in Table 2. Both compounds bind to δ-opioid receptors, which was the main goal of their rational design. DPMPT shows very high binding potency toward δ-opioid receptors with moderate selectivity, whereas DPDMPT shows lower potency, but higher selectivity. No functional assays were performed for DPMPT and DPDMPT. However, since a compound with a similar sequence and 3D structure, Tyr-cyclo(D-Pen-Gly-Trp-L-3-Mpt)-Asp-Phe-NH_2, was shown to be a moderate δ-agonist (Nikiforovich et al., submitted for publication), it is reasonable to assume that, at least, DPMPT would be a δ-agonist.

Conformations of DPDMPT: NMR, Energy Calculations, and X-ray Studies

NMR Spectroscopy of DPDMPT in DMSO. The NMR data for both analogs are presented in Table 3 (^{1}H-NMR spectroscopy data) and Table S1 in the supporting information (^{13}C-NMR spectroscopy data). Figure 2 contains a representative example of ROESY spectra for DPDMPT. (The corre-

(26) Mosberg, H. I.; Omnaas, J. R.; Medzihradsky, F.; Smith, C. B. *Life Sci.* **1988**, *43*, 1013−1020.

(27) Nikiforovich, G. V.; Kolodziej, S. A.; Nock, B.; Bernad, N.; Martinez, J.; Marshall, G. R. *Biopolymers* **1995**, *33*, 439−452.

Table 3. ^{1}H Chemical Shifts (δ, ppm) and Coupling Constants (J, Hz) for DPDMPT (A) and DPMPT (B) (T = 305 K, DMSO-d_6)[a]

	NH		H^α		H^β		H^γ		H^δ	
residue	A	B	A	B	A	B	A	B	A	B
Tyr[1]			4.22 $J(\alpha\beta) = 6.3$ $J(\alpha\beta') = 8.3$	4.23 $J(\alpha\beta) = 6.8$ $J(\alpha\beta') = 8.3$	2.93 β 2.73 β' $J(\beta\beta') = 14.1$	2.93 β 2.73 β' $J(\beta\beta') = 14.1$				
D-Pen[2]	8.41 $J(NH\alpha) = 8.3$ (8.1)	8.64 $J(NH\alpha) = 6.1$ (7.4)	4.49	4.46			1.64 γ 0.91 γ'	1.21 γ 1.05 γ'		
Gly[3]	8.41 $J(NH\alpha) = 9.8$ $J(NH\alpha') = 2.2$ (4.9)	8.90 $J(NH\alpha) = 7.8$ $J(NH\alpha') = 4.8$ (1.3)	4.43 α 3.00 α' $J(\alpha\alpha') = 14.9$	4.16 α 3.08 α' $J(\alpha\alpha') = 14.1$						
Phe[4]	9.10 $J(NH\alpha) = 9.8$ (6.3)	8.21 $J(NH\alpha) = 9.0$ (11.8)	4.86 $J(\alpha\beta) = 6.0$ $J(\alpha\beta') = 9.1$	4.88 $J(\alpha\beta) = 6.8$ $J(\alpha\beta') = 7.8$	3.00 β 2.80 β' $J(\beta\beta') = 14.4$	3.01 β 2.80 β' $J(\beta\beta') = 13.9$				
3-Mpt[5]			5.02 $J(\alpha\beta) = 0.0$	4.38 $J(\alpha\beta) = 0.0$	3.43	3.52	2.07 γ 1.96 γ'	2.30 γ 2.08 γ'	3.36 δ 3.27 δ'	3.92 δ 3.51 δ'

[a] Chemical shifts of Tyr and Phe aromatic protons are 6.69/7.10 and 7.1−7.4 ppm, respectively. Temperature coefficients of NH protons (−ppb/K) are given in parentheses. Chemical shifts are referenced to the solvent signal (2.49 ppm).

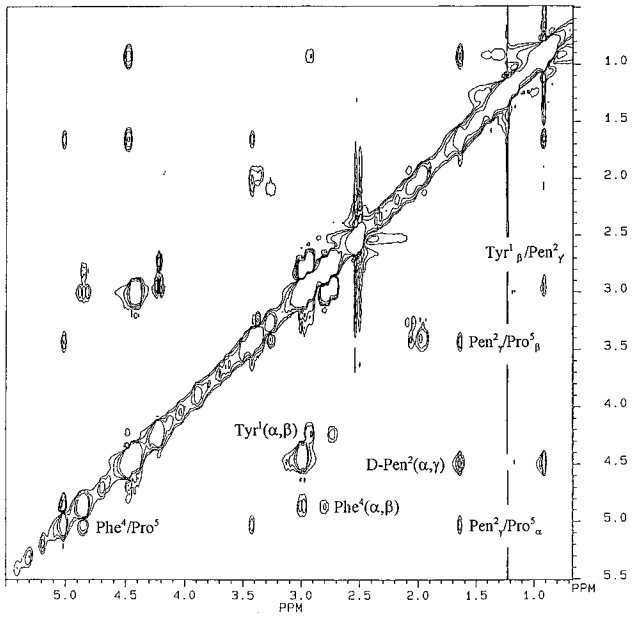

Figure 2. Fragment of the 2D ROESY spectrum for DPDMPT.

sponding example of TOCSY spectra is presented in the supporting information, Figure S1.) In spite of the presence of a proline residue, the presence of a single stable conformer in DMSO-d_6 on the NMR time scale was indicated by the occurrence of well-resolved sharp signals, and the strong ROE contact observed between the Phe αH and D-3-Mpt αH protons suggested that the geometry of the proline amide bond was used in the *cis*-conformation. In addition, other NMR data, including the large (8.3−9.8 Hz) vicinal ^3J(HNC$^\alpha$H) couplings of residues 2−4 as well as the large chemical shift difference ($\Delta\delta$ = 1.4 ppm) of the Gly αH protons, were also indicative of a well-defined solution conformation for the cyclic moiety. From the characteristic chemical shift, couplings, and ROE patterns observed for the Gly αH protons, we were able to deduce their stereospecific assignment. Namely, the Gly α′H proton showing strong ROE and small vicinal coupling with Gly NH was assigned as *pro-R*, while Gly αH showing very weak ROE and large vicinal coupling with Gly NH was assigned as *pro-S*. It is well known that the temperature dependence of the amide proton chemical shift gives valuable information about the existence of hydrogen bonding or solvent-shielded groups. The temperature coefficients of the NH protons in DPDMPT, which are reported in Table 3, namely, the large upfield shifts observed for all the amide protons as the temperature increased, demonstrated that they were all exposed to the solvent and not involved in hydrogen bonding.

The populations of side chain rotamers of the Tyr and Phe residues were quantitatively assessed from the homonuclear J(HC$^\alpha$C$^\beta$H) coupling constants using the Pachler equations[28,29] with Cung's parametrization[30] proposed for aromatic amino acids. The stereospecific assignment of the Phe βH protons could be deduced from the ROE pattern. The population distribution of the Phe side chain showed a slight preference for the $\mathbf{g}^-$ rotamer in accordance with one larger (9.1 Hz) and one smaller (6.0 Hz) coupling constant measured between the corresponding αH and βH protons, and with the medium ROE contacts observed between the different βH protons and NH and αH protons, respectively. However, the contribution of the other two rotamers (**t** and $\mathbf{g}^+$) could also be established. As for Tyr, the preference of the **t** rotamer could be assumed on the basis of the ROE contacts observed between the D-Pen γ'H and Tyr βH/Tyr-Ar- protons, respectively (see Figure 2). The large chemical shift difference of the D-Pen methyl protons could also be rationalized by the anisotropic shielding effect of the Tyr aromatic ring. However, in analogy to Phe, the presence of the other two staggered conformers in dynamic equilibrium could not be excluded.

The ROE correlations of the D-Pen methyl protons, namely, a weak ROE between the Pen γ'H and D-Pen NH and a medium ROE between the D-Pen γH and Gly NH, as well as long-range ROEs between D-Pen γH and D-3Mpt αH/βH protons, allowed the stereospecific assignment of the D-Pen methyls, and, moreover, we could predict the preference of the $\mathbf{g}^-$ rotamer of the D-Pen side chain with $\chi_1 = -60°$ and, accordingly, with the C$^\beta$−S−S−C$^\beta$ angle of −90° (i.e., with the left-handed disulfide bridge). This conformation is also in agreement with the ROE correlations of similar intensities observed between the D-Pen αH and D-Pen γH/D-Pen γ'H protons, respectively. Thus, in the proposed conformation the D-Pen γ-methyl group points toward the 14-membered ring and is in the *gauche* arrangement with respect to the D-Pen carbonyl, while the D-Pen γ'-methyl points away from the cycle and is in the *gauche* position to the D-Pen amide. This conformation was also in excellent agreement with the observed carbon chemical shift difference ($\Delta\delta$ = 1.8 ppm) of the D-Pen methyl carbons.

(28) Pachler, K. G. R. *Spectrochim. Acta* **1963**, *19*, 2085−2092.
(29) Pachler, K. G. R. *Spectrochim. Acta* **1964**, *20*, 581−587.
(30) Cung, M. T.; Marraud, M. *Biopolymers* **1982**, *21*, 953−967.

Table 4. Experimental ROEs vs Calculated Interproton Distances in DPDMPT Conformers **A**, **B**, **C**, and **D**

interproton contact	experimental ROE	interproton distances (Å)			
		A	**B**	**C**	**D**
D-Pen NH−D-Pen γ' CH_3	weak	3.64	2.80	3.63	2.80
D-Pen NH−Tyr αH	medium/strong	2.24	2.25	2.39	2.39
D-Pen NH−D-Pen αH	medium	2.91	2.83	2.91	2.83
Gly NH−D-Pen αH	strong	2.35[a]			
Gly NH−Gly α′H	strong	2.47[a]			
Gly NH−Gly αH	weak	2.96[a]			
Gly NH−D-Pen γCH_3	medium	2.86[a]			
Phe NH−Gly αH	strong	2.22[a] (3.25 for Gly α′H)			
Phe NH−Phe αH	weak	2.88[a]			
D-Pen αH−D-Pen γCH_3	medium	2.79[a]			
D-Pen αH−D-Pen $\gamma' CH_3$	medium	2.67[a]			
D-3-Mpt αH−Phe αH	medium/strong	2.16[a]			
D-3-Mpt αH−D-3-Mpt βCH_2	weak/medium	2.79[a]			
D-3-Mpt αH−D-Pen γCH_3	weak/medium	2.96[a]			
D-3-Mpt βCH_2−D-Pen γCH_3	weak/medium	3.51[a]			

[a] For all structures.

Considering the γ-substituent effects[31,33] of the NH ($\Delta\delta = -5.1$ ppm, shielding parameter) and CO ($\Delta\delta = -3.2$ ppm) groups in the *gauche* position with respect to the relevant D-Pen methyl carbons, the preference of the $\mathbf{g}^-$ rotamer could also be confirmed. (In addition, assuming the dominance of the $\mathbf{g}^-$ rotamer, the reference carbon chemical shift of the D-Pen methyl carbons could be predicted. Its value, in turn, could be used for quantitative evaluation of the D-Pen side chain conformation in the other (DPMPT) analog.) However, on the basis of the available NMR data, we could not exclude the presence of a conformational equilibrium between different values of the ϕ dihedral angle for the D-Pen residue.

In conclusion, one conformer of the cyclic moiety with a *cis*-proline amide bond was deduced from the NMR data. As for the acyclic part, it was suggested to be rather flexible, which is in perfect agreement with theoretical results (see below).

Energy calculations performed with $\epsilon = 45$ (see the Experimental Section) revealed 31 low-energy ($E - E_{min} \leq 5$ kcal/mol) different backbone conformers of DPDMPT. In all the conformers the *cis*-conformation of the mercaptoproline-preceding peptide bond was energetically preferable over the *trans*-conformation, which is in excellent agreement with NMR observations. The values of $J(HNC^{\alpha}H)$ vicinal constants and interproton distances were calculated for each conformer. Comparison with the structural parameters measured by NMR showed that four of the DPDMPT low-energy structures meet the requirements of matching the experimental vicinal constants ($|J_{exptl} - J_{calcd}| \leq 1$ Hz) and estimations of the ROEs within the peptide backbone (Table 4). Note that some of the distances in Table 4 were not calculated between protons, but included the united atomic centers of the CH_n type (see the Experimental Section).

The four low-energy conformers in question are described in Table 5. It is obvious that all of them have the same backbone conformer of the cyclic moiety, since the only differences are in the values of dihedral angles outside the cyclic moiety. The available experimental data do not suggest any particular conformer out of these to be the DPDMPT solution conformation. Each of them is a possible candidate for a single conformer model. However, DPDMPT may exist in DMSO solution in conformational equilibrium among several backbone conformations with the same type of 3D structure for the cyclic moiety, but with somewhat different conformers of the acyclic part of the molecule. Conformers **A**, **B**, **C**, and **D**, which are listed in Table 5, are also depicted in Figure 3, where the conformational equilibrium in question might be readily seen. It is noteworthy that all these conformers possess two additional close interproton contacts, namely, Gly α′H−Phe NH and D-3-Mpt αH−Phe NH, which are not observed in the experimental ROESY spectra.

Table 5. Low-Energy Conformers of DPDMPT Compatible with Experimental Data by NMR Spectroscopy

	Tyr	D-Pen		Gly		Phe		D-3-Mpt	
	ψ	ϕ	ψ	ϕ	ψ	ϕ	ψ	ω	ϕ
A	138	141	−151	123	−124	−153	67	14	75
B	140	73	−146	123	−125	−153	66	13	75
C	80	142	−151	127	−121	−155	66	13	75
D	80	73	−146	123	−125	−153	66	12	75
X-ray	124	127	−140	114	−126	−127	69	6	86

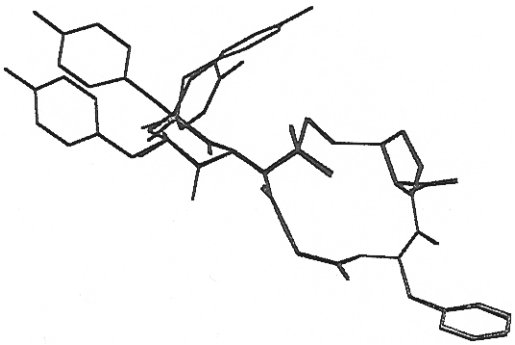

Figure 3. Overlapping of four possible conformers of DPDMPT in DMSO solution. All hydrogens are omitted.

Additional energy calculations were performed with the assumption of $\epsilon = 45$ to reveal conformational flexibility of the Tyr and Phe side chains of DPDMPT (see the Experimental Section). Totally, 123 low-energy conformers were selected as different both in their backbone conformers and in the rotamers of the side chains in question. Among them, 16 belong to the **A** type of backbone conformation, 17 to **B**, 4 to **C**, and 4 to **D**. Within these 41 conformers, the distributions over $\mathbf{g}^+$, **t**, and $\mathbf{g}^-$ rotamers (in percents) were as follows: 0.19, 0.41, and 0.40 for the Tyr residue, and 0.02, 0.46, and 0.52 for the Phe residue. These numbers are in good agreement with those estimated by NMR measurements. They strongly suggest conformational equilibrium among different rotamers with **t** and $\mathbf{g}^-$ rotamers as most populated for both residues in question.

(31) Grant, D. M.; Cheney, B. V. *J. Am. Chem. Soc.* **1967**, *89*, 5315−5318.
(32) Hansen, P. E.; Batchelor, J. G.; Feeney, J. *J. Chem. Soc., Perkin Trans. 2* **1977**, *1*, 50−54.
(33) Wolfenden, W. R.; Grant, D. M. *J. Am. Chem. Soc.* **1966**, *88*, 1496−1502.

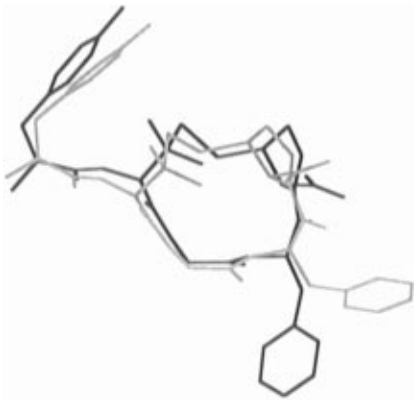

Figure 4. X-ray structure of DPDMPT (in bold) overlapped with the **A** conformer of DPDMPT in DMSO solution (ligher lines). All hydrogens are omitted.

The X-ray study was performed for DPMPT·ETOH. In the crystal each peptide molecule is linked through hydrogen bonding to four other peptide molecules (see Table S2 in the supporting information). All of the N···O peptide—peptide bonds are to the nearest neighbors along the *b* cell axis. There is also a CH···O=C hydrogen bond in DPMPT between $C1^{\alpha}$ and C=O3 of a neighboring molecule which forms a link similar to the three N···O bonds. The geometric parameters (see Table S2) for this bond fall well within the bounds described by Jeffrey[34] for this type of interaction. The remaining peptide—peptide bonds are of a "head to tail" type linking $O1^{\zeta}$ and the CO^{-}-terminus along the *a* cell axis direction. There is a second head to tail connection which links N1 and the C-terminus of a neighboring molecule through an ethanol bridge (N1···O1S···C=O5 and N1···O2S···CO^{-}).

The X-ray structure of DPDMPT is shown in Figure 8 and partly described as a last entry in Table 5 (for a full description, see the Discussion). The X-ray structure shows remarkable similarity to the DPDMPT solution conformations, being most close to the **A** conformer (see Figure 4). In the X-ray structure of DPDMPT, the Tyr residue is folded back toward the peptide cyclic moiety, which corresponds to the **t** rotamer of the Tyr side chain. Also, the X-ray structure confirms a *cis*-conformation of the peptide bond, which precedes the D-3-Mpt residue. Generally, the entire conformational data obtained for DPDMPT by energy calculations, NMR spectroscopy, and X-ray crystallography are in exceptionally good agreement with each other.

Conformations of DPMPT: NMR and Energy Calculations

NMR Spectroscopy of DPMPT in DMSO. In contrast to DPDMPT, the strong ROE observed between the Phe αH and L-Mpt δH protons indicated a *trans*-peptide bond in the DPMPT analog in DMSO solution. However, to explain all long-range ROE correlations observed between the D-Pen and L-Mpt residues, we should assume a dynamic equilibrium of two 3D structures with identical backbone conformations but with different side chain rotamers of D-Pen with χ_1 values of −60° (**g**$^{-}$) and 180° (**t**), respectively, and, accordingly, with different helicity of the disulfide bridge with the $C^{\beta}-S-S-C^{\beta}$ angle values of +90° and −90°, respectively. The population of these fastly interconverting conformers could be predicted from the carbon chemical shifts of the D-Pen methyl carbons considering the γ-substituent effects of NH and CO groups and using the reference carbon chemical shift derived from the analysis of the other analog (see above). It was found that the D-Pen side chain most likely adopts the **g**$^{-}$ conformation (60−70% of the population), whereas the *trans*-conformation is populated up to 30−40%. These data are in excellent agreement with calculation results (see below) and can also be qualitatively confirmed by other NMR data. For example, the long-range ROE correlations observed between the D-Pen γH and L-Mpt γH/δH protons could be explained by the presence of the conformer of D-Pen with $\chi_1 = -60°$, whereas the medium ROE observed between the D-Pen γ′H and L-Mpt αH protons could only be rationalized by the existence of the other structure with $\chi_1 = 180°$ of D-Pen. This latter conformation is also consistent with the low temperature gradient of the Gly amide proton, since the NH group pointing toward the cycle becomes significantly shielded from the solvent. The relatively broad NH signals of the Gly and Phe residues observed at room temperature are also indicative of the presence of some kind of conformational equilibrium. As expected, those signals become considerably sharper as the temperature increases due to the enhancement of the interconversion rate between different conformers. This feature of the NH signals was exploited in the ROE experiment at elevated temperature to reveal all possible ROE contacts.

The NMR parameters of the Gly residue being different from those in the other analog [$J(HNC^{\alpha}H)$ = 7.8 and 4.8 Hz, $^{1}J(C^{\alpha}H^{\alpha})$ = 141.4 and 142.3 Hz, respectively] were also indicative of different backbone conformations of the two analogs. However, a very similar population distribution of side chain rotamers could be predicted for both Tyr and Phe residues compared to the corresponding populations for the DPDMPT analog, indicating that the side chain conformations are not significantly influenced by the change in chirality of the Mpt residue. Also, as in the DPDMPT analog, the flexibility of the acyclic part due to rotations around the $HNC^{\alpha}H$ bond of D-Pen (φ rotamers) could not be excluded on the basis of the available NMR data.

In summary, a dynamic equilibrium of two conformers differing in their χ_1 angles for the D-Pen residue was predicted from NMR data. This conformational equilibrium, which occurs fast on the NMR time scale, allowed us to explain all available experimental NMR data, and is also consistent with calculations. The high mobility of the acyclic part predicted from NMR data was also in accordance with the results of calculations.

Energy calculations performed with $\epsilon = 45$ (see the Experimental Section) revealed 22 low-energy ($E - E_{min} \leq 5$ kcal/mol) different backbone conformers of DPMPT. In contrast with the case of DPDMPT, for all low-energy conformers of DPMPT the *trans*-conformation of the mercaptoproline-preceding peptide bond was energetically preferable over the *cis*-conformation, which, again, is in excellent agreement with the NMR data. The values of $J(HNC^{\alpha}H)$ vicinal constants and interproton distances were calculated for each of the low-energy conformers. Comparison with the structural parameters measured by NMR showed that no single DPMPT low-energy structure meets the requirements of matching the experimental vicinal constants ($|J_{exptl} - J_{calcd}| \leq 1$ Hz) and the intrabackbone ROE estimations simultaneously. However, it is possible to select six conformers with minimal violations of the above requirements. These conformers are compared to the experimental ROEs in Table 6; the discrepancies between experimental and calculated values are shown in italics.

The data of Table 6 show that the agreement between NMR data and the results of calculations may be easily achieved assuming conformational equilibrium occurs among the six low-energy conformers of DPMPT, which are mentioned in Table 6. It is obvious that in this case the absence of observed

(34) Jeffrey, G. A.; Saenger, W. *Hydrogen Bonding in Biological Structures*; Springer-Verlag: New York, 1991; pp 156−160.

Table 6. Experimental ROEs vs Calculated Interproton Distances in DPMPT Conformers **A**, **B**, **C**, **D**, **E**, and **F**

interproton contact	experimental ROE	interproton distances (Å)					
		A	**B**	**C**	**D**	**E**	**F**
D-Pen NH−Tyr αH	medium	2.25	2.25	2.25	2.39	2.39	2.25
Gly NH−D-Pen αH	strong	2.35	2.37	2.30	2.36	2.37	2.31
Gly NH−Gly α′H	medium/weak	2.27	2.27	2.29	2.28	2.27	2.29
Gly NH−D-Pen γCH_3	weak	2.87	2.79	*4.60*	2.84	2.79	*4.57*
Phe NH−Gly αH	weak	2.53	2.54	2.68	2.54	2.54	2.68
Phe NH−Phe αH	weak	2.92	2.92	2.93	2.92	2.92	2.93
D-3-Mpt αH−D-Pen $\gamma'CH_3$	medium	*5.72*	*5.70*	3.13	*5.74*	*5.70*	3.09
D-3-Mpt δCH_2−D-Pen γCH_3	weak	3.65	3.63	*6.17*	3.67	3.63	*6.13*
D-3-Mpt γCH_2−D-Pen γCH_3	weak	3.32	3.35	*5.77*	3.34	3.34	*5.74*
D-Pen αH−D-Pen $\gamma'CH_3$	medium	2.75	2.73	3.44	2.75	2.73	3.44
D-Pen αH−D-Pen γCH_3	medium	2.71	2.73	2.78	2.71	2.73	2.77

Table 7. Low-Energy Conformers of DPMPT Most Compatible with Experimental Data by NMR Spectroscopy

	Tyr	D-Pen			Gly		Phe		L-3-Mpt	
	ψ	ϕ	ψ	$\chi 1$	ϕ	ψ	ϕ	ψ	ω	ϕ
A	140	76	−146	−66	80	−73	−136	74	−178	−75
B	140	140	−149	−63	80	−72	−136	75	−178	−75
C	140	81	−139	169	85	−59	−130	74	−170	−75
D	80	73	−147	−66	81	−72	−138	73	−177	−75
E	80	140	−149	−63	80	−72	−136	75	−178	−75
F	140	137	−141	170	85	−59	−129	74	−170	−75

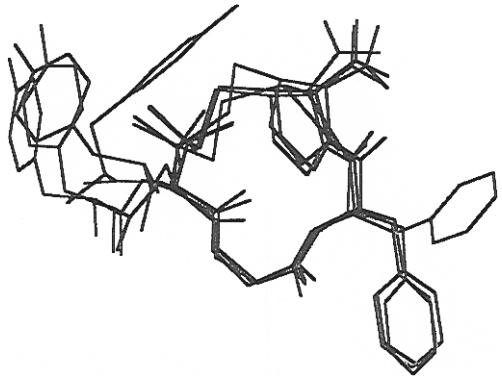

Figure 5. Overlapping of four representative possible conformers of DPMPT in DMSO solution. All hydrogens are omitted.

interproton contacts in one of the conformers would be compensated by their presence in others. The assumption seems even more likely, since all six conformers represent the same 3D structure of the backbone of the cyclic moiety, the differences being in the values of backbone dihedral angles outside the cyclic moiety and in rotamers of the D-Pen side chain (see Table 7). Therefore, it could be postulated that DPMPT exists in DMSO solution in conformational equilibrium among several backbone conformations with the same type of 3D structure for the cyclic moiety, but with somewhat different conformers of the acyclic part of the molecule and two types of rotamers for the D-Pen side chain. Representative conformers **A**, **C**, **D**, and **F** are depicted in Figure 5, where conformational equilibrium is readily seen. As in the case of DPDMPT, it is noteworthy that some of the conformers, namely, **C** and **F**, possess the additional close interproton contacts, namely, D-Pen γCH_3−Phe NH and D-Pen NH−D-Pen $\gamma/\gamma'CH_3$, which are not observed in the experimental ROESY spectra.

The conformational flexibility of the Tyr and Phe side chains of DPMPT was investigated in the same way as in the case of DPDMPT (see the Experimental Section). Totally, 79 low-energy conformers were selected as different both in their backbone conformers and in the rotamers of the side chains in question. Among them, 23 belong to conformers **A**−**F**. Within these 23 conformers, the distributions over $\mathbf{g}^+$, **t**, and $\mathbf{g}^-$ rotamers (in percent) were as follows: 0.22, 0.48, and 0.30 for the Tyr residue, and 0.13, 0.39, and 0.48 for the Phe residue. Again, these numbers are in good agreement with those estimated by NMR measurements for DPMPT. Note also that for the six conformers of Table 7, which are presumably interconverting into each other in DMSO solution, the $\mathbf{g}^-$ rotamer of the D-Pen residue is represented twice as much as the **t** rotamer. This finding is also in good agreement with NMR data.

Generally, it could be concluded that by combining the independent studies of DPMPT by energy calculations and NMR spectroscopy, we produced a realistic description of DPMPT solution conformation. Unfortunately, the X-ray data on DPMPT were not obtained, since the corresponding crystals were not available.

Discussion

DPMPT and DPDMPT were both designed to meet two main requirements: (i) to obtain a rigidified DPDPE analog and (ii) to be compatible with the model of the δ-receptor-bound DPDPE conformer proposed earlier. The second requirement was fulfilled for both analogs, as was shown above. However, DPMPT is 30-fold more potent in binding to δ-opioid receptors than DPDMPT. Since we have determined solution conformations of both compounds, we can compare them to those matching the δ-receptor-bound conformer of DPDPE (Table 1). In this comparison, we have calculated the RMS values for the atomic centers, which were used initially for deducing the model itself, namely, the nitrogen atom of the α-amino group, the C^γ and C^ζ atoms of the Tyr and the Phe aromatic rings, and the C^α atom of the D-Pen[2] residue. It was assumed also that rotamers of the side chains of the Tyr and Phe residues correspond to **t** and $\mathbf{g}^-$, respectively.

Results of comparison showed that all four of the possible solution conformations of DPDMPT (Table 5) overlap with the suggested δ-receptor-bound conformations of DPDMPT (Table 1) with RMS values greater than 1.5 Å, the lowest one being for the **A** conformer (RMS = 1.55 Å). At the same time, two of the six possible solution conformations of DPMPT, namely, the **C** and **F** conformers (Table 7), are compatible with the suggested δ-receptor-bound conformation of DPMPT (Table 1) with RMS 0.83 Å. Both cases of overlappings are depicted in Figure 6. This finding can explain the difference in binding of DPMPT and DPDMPT to δ-receptors by a simple suggestion that the δ-receptor-bound conformation of DPMPT already preexists in solution, whereas solution conformations of DPDMPT should be more significantly distorted to match the δ-receptor-bound conformation of DPDMPT. Note that this suggestion tacitly assumes the similarity of DPMPT and DPDMPT conformations in DMSO and water, which has been pointed out in the case of the more flexible DPDPE.[4]

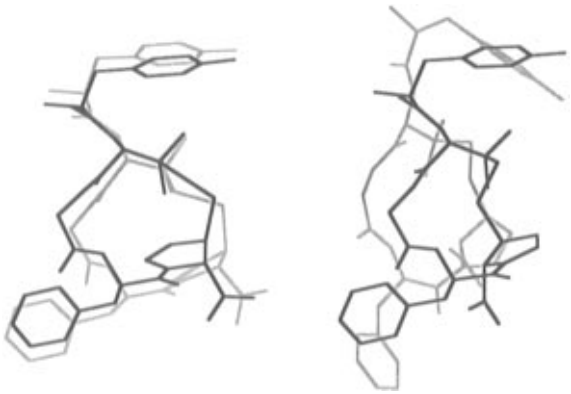

Figure 6. Best overlappings of suggested δ-receptor-bound conformers (in bold) with one of the conformers in DMSO solution (lighter lines) for DPMPT (left) and DPDMPT (right). All hydrogens are omitted.

DPMPT and DPDMPT also showed different levels of δ/μ-selectivity. DPDMPT possesses a greater selectivity, since it practically does not bind μ-opioid receptors. On the contrary, DPMPT binds μ-opioid receptors with reasonable potency. While it is almost impossible to discuss reasons for nonbinding of DPDMPT to μ-opioid receptors (there are just too many), it is possible to point out at least one reason why DPMPT could bind μ-opioid receptors. It was shown that the ability of DPDPE analogs to distinguish between δ- and μ-opioid receptors depends on the presence of bulky methyl substituents of the C^{β} atom in the C-terminal residue; i.e., the analogs with the Cys[5] residue more effectively bind μ-opioid receptors than the analogs with the Pen[5] residue (see, e.g., ref 35). The same trend was observed in recent studies of cyclic analogs of deltorphins[36] as well as for DPLPE−deltorphin chimeric peptides.[37] In the case of DPMPT, only one bulky substituent of the C^{β} atom in question is present instead of two as in DPDPE (see Figure 1). Therefore, it would be reasonable to assume that the presence of the second bulky substituent makes it difficult for an analog to bind μ-opioid receptors. This assumption could be verified experimentally, if stereospecifically β-methylated derivatives of the Cys residue are available.

Since DPMPT and DPDMPT are closely related to DPDPE, it is natural to compare their conformers with those of DPDPE itself. Conformations of DPDPE were studied repeatedly by molecular modeling, NMR spectroscopy, and X-ray crystallography (see references in the Introduction). Several models were suggested for DPDPE solution conformations in DMSO[4,38] and water.[3,4,12,38] We have collected all available data on suggested models of DPDPE conformers in solution and compared them to DPMPT and DPDMPT conformers in DMSO proposed in this study (Tables 9 and 6, respectively). For this comparison, we have calculated the RMS values for all C^{α} and C^{β} atoms, i.e., for the atomic centers, which are rigidly attached to the peptide backbone.

Comparison showed that two conformers, suggested for DPDPE in DMSO solution by NMR spectroscopy with the subsequent run of restricted molecular dynamics (structure III′ in ref 4) and by combined independent use of NMR spectroscopy and molecular modeling (structure 4 in ref 38), are quite similar to the **F** conformer of DPMPT (the RMS values are 0.76 and 0.69 Å, respectively). This similarity is illustrated by Figure 7. Another DPMPT conformer, **B**, is similar to X-ray structures of DPDPE(1) and -(3) (see Table 8), the RMS values being 0.82 and 0.89 Å, respectively. At the same time, none of the DPMPT conformers in Table 7 are similar to the DPDPE solution conformation in water, which was suggested earlier.[3] Also, none of the DPDMPT conformers listed in Table 5 showed similarity to any of the suggested DPDPE solution conformers. However, the **A** conformer of DPDMPT is similar to the DPDPE(3) X-ray structure (RMS 0.96 Å). Generally, it can also be concluded that DPMPT is closer to DPDPE than DPDMPT at the level of solution conformations.

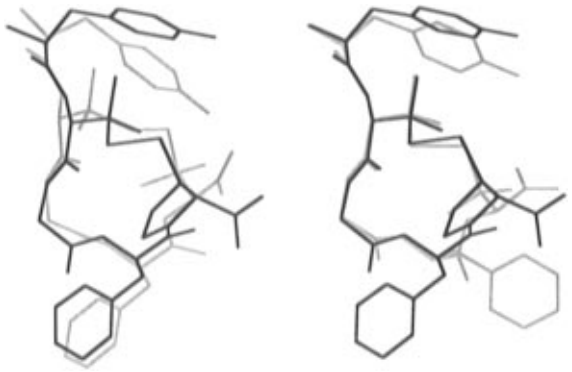

Figure 7. **F** conformer of DPMPT in DMSO solution (in bold) overlapped with suggested conformers of DPDPE in DMSO solution by other authors (lighter lines): ref 4 (left) and ref 38 (right). All hydrogens are omitted.

Table 8. Selected Torsion Angles for DPDMPT and DPDPE in Crystalline Form[a]

		DPDMPT	DPDPE(1)	DPDPE(2)	DPDPE(3)
Tyr[1]	ψ	124	−157	9	−175
	ω	−174	−179	172	−175
	χ_1	−171	−68	−71	−61
	χ_2	53	118	99	127
D-Pen[2]	φ	127	110	129	129
	ψ	−140	−147	−152	−145
	ω	−173	−171	−175	−173
Gly[3]	φ	114	98	107	99
	ψ	−126	−141	−138	−138
	ω	−178	−178	−180	−178
Phe[4]	φ	−127	−74	−76	−81
	ψ	69	−36	−30	−18
	ω	6	−175	−175	−170
	χ_1	−63	−67	−67	−69
	χ_2	−87	−85	−80	−85
3-D-Mpt[5]	φ	86	126	116	106
	N−C^{α}−C^{β}−C^{γ}	−42			
	C^{α}−C^{β}−C^{γ}−C^{δ}	36			
S−S bridge					
	N5−$C5^{\alpha}$−$C5^{\beta}$−S5	77	−51	−46	−52
	$C5^{\alpha}$−$C5^{\beta}$−S5−S2	140	174	176	168
	$C5^{\beta}$−S5−S2−$C2^{\beta}$	−84	−105	−108	−104
	S5−S2−$C2^{\beta}$−$C2^{\alpha}$	−77	−73	−73	−74
	S2−$C2^{\beta}$−$C2^{\alpha}$−C2′	54	69	62	69

[a] Note: In DPDPE residue 5 is D-Pen.

The X-ray structure of DPDMPT obtained in this study is somewhat different from those of DPDPE. The X-ray structure of DPDPE[14] contained three independent peptide molecules in the asymmetric unit. All three unique molecules showed essentially the same ring conformation, but two different orientations were found for the Tyr side chain. In DPDMPT the conformation of the 14-membered ring, at residues 2, 3, and 4, and the orientation of the Phe side chain are similar to those found in DPDPE itself (see Figure 8 and Table 8) with the best agreement being for residues 2 and 3. The most significant differences between the two structures lie in the

(35) Mosberg, H. I.; Schiller, P. W. *Int. J. Pept. Protein Res.* **1984**, *23*, 462−466.
(36) Misicka, A.; Lipkowski, A. W.; Horvath, R.; Davis, P.; Yamamura, H. I.; Porreca, F.; Hruby, V. J. *J. Med. Chem.* **1994**, *37*, 141−145.
(37) Misicka, A.; Lipkowski, A. W.; Horvath, R.; Davis, P.; Porecca, F.; Yamamura, H. I.; Hruby, V. J. *Int. J. Pept. Protein Res.* **1994**, *44*, 80−84.
(38) Nikiforovich, G. V.; Prakash, O. M.; Gehrig, C. A.; Hruby, V. J. *Int. J. Pept. Protein Res.* **1993**, *41*, 347−361.

Table 9. Summary of Crystal Data Parameters

molecular formula (DPDMPT)	$C_{30}H_{37}N_5O_7S_2$
unit cell contents	$2(C_{30}H_{37}N_5O_7S_2)\cdot4(C_2H_6O)$
crystal size (mm)	$0.08 \times 0.22 \times 0.52$
crystal system	monoclinic
space group	$P2_1$
a	10.918(1) Å
b	10.017(2) Å
c	17.378(2) Å
α	90°
β	101.55(1)°
γ	90°
cell volume	1862.1(5) Å^3
density (calcd)	1.31 g/cm^3
absorption coefficient	1.79 mm^{-1}
F(000)	784
radiation	Cu Kα ($\lambda = 1.541\,78$ Å)
θ range for data collection	2.6−56.0°
resolution	0.95 Å
no. of reflections collected	2829
no. of independent reflections	2589 ($R_{int} = 0.030$)
no. of parameters refined	452
final *R* indices (2289 reflections with $I > 2\sigma I$)	$R1 = 0.085$, $wR2 = 0.213$
final *R* indices (all data−9802 reflections)	$R1 = 0.094$, $wR2 = 0.230$
goodness-of-fit on F^2	1.05
largest difference peak and hole	1.5 and −0.65

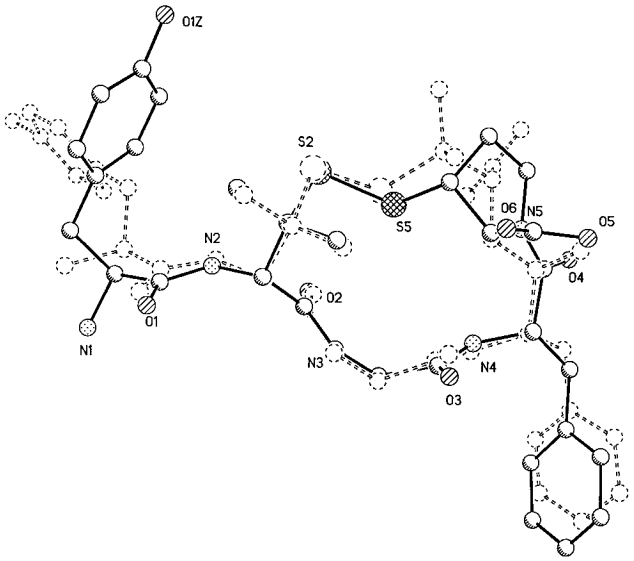

Figure 8. X-ray structure of DPDMPT (solid lines) overlapped with one of the X-ray structures of DPDPE (dashed lines).

orientation of the N- and C-termini. The amide bond of the Tyr residue is *trans* in both structures, but the rotation about the C1$^\alpha$−C1′ bond (described by the ψ torsion) is −157°, +9°, and −175° for the three molecules of DPDPE and is 124° in DPDMPT (Table 8). In the three molecules of DPDPE the Tyr side chain is extended away from the 14-membered ring. In DPDMPT, the Tyr residue is folded back toward the peptide ring which affects distances between N1 and O1$^\zeta$ and the center of the phenolic ring. In DPDPE, the N1···O1$^\zeta$ distances range from 6.4 to 6.5 Å and the N1 to the center of the phenolic ring distances range from 3.0 to 4.0 Å. In DPDMPT these distances are 7.9 and 5.2 Å, respectively. The distance between the centers of the aromatic rings, the N1 to Phe distance, and the angles between the planes of the two aromatic rings in DPDMPT fall within the ranges observed in DPDPE: the ring−ring distance is 13.7 Å in DPDMPT (13.2−15.9 for DPDPE), the N1 to Phe[4] distance is 12.1 Å in DPDMPT (12.3−13.4 in DPDPE), and the angle between the planes is approximately 60° in DPDMPT (46°, 60°, and 132° in DPDPE). In DPDPE all the peptide bonds (ω torsions) are *trans*. In DPDMPT the presence of the proline moiety imposes a *cis*-peptide bond on the preceding residue. In addition, even though residue 5 is a D-residue in both compounds the COO$^-$-terminus lies on the opposite side of the best plane through the 14-membered ring.

Finally, it would be helpful to summarize the most important conclusions of this study. We have designed and obtained a novel conformationally constrained analog with high potency toward *δ*-opioid receptors, DPMPT. Along with it, an analog with a somewhat different profile of interaction with opioid receptors, DPDMPT, was obtained. Both analogs were subjected to a comprehensive conformational analysis, including independent studies by molecular modeling, NMR spectroscopy, and, in the case of DPDMPT, X-ray crystallography. The results of all these independent studies produced remarkably coherent results describing conformations of both analogs. Confronted with the biological data, these results provide the explanation of relative binding potency and selectivity of DPMPT and DPDMPT. They clearly showed that conformational features of DPMPT are closer to those of DPDPE, compared with conformational features of DPDMPT. It is very important also that our results once again strongly confirm and, to some extent, refine the 3D model for the *δ*-opioid pharmacophore, which was proposed earlier by molecular modeling. The last, but not least, outcome of this study is that it opens the way to design *δ*-selective peptidomimetics. Indeed, the use of unnatural chimeric amino acid residues can be regarded as the first step toward transforming the peptide structure of DPDPE into peptidomimetics. Most important, however, is that this transformation might be verified on a permanent basis by the reliable 3D model of the *δ*-opioid peptide pharmacophore.

Experimental Section

Synthesis. General Procedures. The general synthetic methods were identical to those which we have previously published[27,39] with the exception of the following: Merrifield resin (loading 0.78 mequiv/g resin) was purchased from Advanced Chemtech (Louisville, KY). Details of the synthesis are described in the supporting information.

Molecular Modeling. Energy calculations for DPMPT and DPDMPT were performed by use of buildup procedures, similar to those employed previously for other cyclic peptides (see, e.g., ref 15). The ECEPP/2 potential field[41,42] was used assuming rigid valence geometry with planar *trans*-peptide bonds. Both *trans*- and *cis*-conformations were examined for peptide bonds in mercaptoproline residues. (Note that *trans*- and *cis*-mercaptoprolines differ in chirality of the sulfur-substituted carbon, which is independent of *trans*/*cis*-isomerization of mercaptoproline peptide bonds.) Only the ω angles inside the cyclic moieties were allowed to vary. The valence geometry and atomic charges for mercaptoproline residues were calculated by the use of the SYBYL program with the standard TRIPOS force field. Aliphatic and aromatic hydrogens were generally included in united atomic centers of the CH$_n$ type; H$^\alpha$ atoms and amide hydrogens were described explicitly.

The main calculation scheme involved several successive steps. First, the conformational possibilities of cyclic model fragments, Ac-cyclo(D-Pen-Gly-Ala-L/D-3-Mpt)-NMe, were considered (assuming $\epsilon = 2.0$). At this step, all possible combinations of local minima for the peptide backbone for each amino acid residue were considered, i.e., the minima in the Ramachandran map of the ***E****, ***F****, ***C****, ***A***, and ***A**** types (according to the notation in ref 43) for the D-Pen residue, of the ***E***, ***F***, ***C***, and ***A**** types for the Ala residue, of the ***E****, ***F****, ***C****, ***A***, ***E***, ***F***, ***C***, and ***A**** types for the Gly residue, and of the ***F***, ***C***, and ***A*** types for

(39) Kolodziej, S. A.; Nikiforovich, G. V.; Skeean, R.; Lignon, M.-F.; Martinez, J.; Marshall, G. R. *J. Med. Chem.* **1995**, *38*, 137−149.
(40) Bodanszky, M. *The Practice of Peptide Synthesis*; Springer-Verlag: Berlin, 1984.
(41) Nemethy, G.; Pottle, M. S.; Scheraga, H. A. *J. Phys. Chem.* **1983**, *87*, 1883−1887.
(42) Dunfield, L. G.; Burgess, A. W.; Scheraga, H. A. *J. Phys. Chem.* **1978**, *82*, 2609−2616.
(43) Zimmerman, S. S.; Scheraga, H. A. *Biopolymers* **1977**, *16*, 811−843.

mercaptoprolines. For each backbone conformation, one optimal possibility to close a cycle employing the parabolic potential functions, intrinsic to the ECEPP force field, was found by checking an energy profile of rotation around the dihedral angle χ_1 for the D-Pen residue. Totally, 960 conformations for each of the cyclic moieties were considered. Then, the conformers satisfying the $E - E_{min} < \Delta E = 10$ kcal/mol criterion and differing by more than 40° in at least one value of any backbone dihedral angle (225 and 262 conformers for DPMPT and DPDMPT, respectively) were selected for the next step, which was the conformational analysis of DPMPT and DPDMPT themselves. All local minima of the ***E***, ***C***, and ***A*** types for the N-terminal Tyr residue were considered. The total numbers of conformers considered were 675 and 786 for DPMPT and DPDMPT, respectively. The dihedral angle values of the Tyr and Phe side chain groups and of the terminal groups of the backbone were optimized before energy minimization to achieve their most favorable spatial arrangements, employing an algorithm previously described.[15] Starting from this step, all calculations were performed independently for the values of the dielectric constant $\epsilon = 2.0$ (the standard value for the ECEPP/2 force field) and $\epsilon = 45$ (the macroscopic ϵ value for DMSO); first, the calculations with $\epsilon = 2.0$ will be described.

A total of 394 and 484 conformers for DPMPT and DPDMPT, respectively, out of those considered satisfied the $\Delta E = 10$ kcal/mol criterion. Again, only conformers differing by more than 40° in at least one value of any backbone dihedral angle or by the dihedral angle χ_1 for the D-Pen residue were selected. At the level of the $\Delta E = 5$ kcal/mol criterion, this selection yields 20 and 25 low-energy conformers for DPMPT and DPDMPT, respectively. In the final step, all different rotamers of the χ_1 dihedral angles for the Tyr and Phe residues (i.e., the $\mathbf{g}^+$, **t**, and $\mathbf{g}^-$ rotamers) was considered separately for selected conformers of DPMPT and DPDMPT. This step yields 49 and 85 low-energy conformers ($\Delta E = 5$ kcal/mol) which are different by dihedral angles of the backbone and by all χ_1 angles, for DPMPT and DPMPT, respectively.

In calculations performed with $\epsilon = 45$, 113 and 139 conformers for DPMPT and DPDMPT, respectively, out of those considered satisfied the $\Delta E = 5$ kcal/mol criterion after the first step of calculations. The selection of conformers differing by more than 40° in at least one value of any backbone dihedral angle or by the dihedral angle χ_1 for the D-Pen residue yields 22 and 31 low-energy conformers at the level of the $\Delta E = 5$ kcal/mol criterion, for DPMPT and DPDMPT, respectively. In the final step, again, all different rotamers of the χ_1 dihedral angles for the Tyr and Phe residues (i.e., the $\mathbf{g}^+$, **t**, and $\mathbf{g}^-$ rotamers) were considered separately for selected conformers of DPMPT and DPDMPT. This step yields 79 and 123 low-energy conformers ($\Delta E = 5$ kcal/mol) which are different by dihedral angles of the backbone and by all χ_1 angles, for DPMPT and DPDMPT, respectively.

Geometrical Comparison. The best fit in the superposition for the atomic centers in a pair of conformers was assessed to check the level of geometrical similarity between the two conformers, according to ref 44. The details of the procedure are given in the supporting information.

NMR Measurements. All homo- and heteronuclear NMR experiments were carried out at 305 K, unless otherwise noted, with a Bruker AC-400 spectrometer (400 MHz proton, 100 MHz carbon frequency) equipped with an ASPECT-3000 computer and a 5 mm inverse probehead. Peptide samples were dissolved in DMSO-d_6 at a concentration of 16.2 mg/0.5 mL and 13.7 mg/0.5 mL for DPDMPT and DPMPT, respectively. To account for a possible self-aggregation of peptides, NMR spectra were rerecorded after 10−15-fold dilution with no visible changes observed. Chemical shifts were referenced to the DMSO-d_6 solvent signal at 2.49 ppm for ^{1}H and 39.5 ppm for ^{13}C.

The NMR parameters used in the present study were obtained from 1D and 2D experiments. Five 1D proton spectra were recorded at 5 K intervals from 305 to 325 K to measure the NH temperature coefficients, $\Delta\delta/\Delta T$. Sequential assignment[45] of proton resonances was achieved by the combined use of 2D total correlated spectroscopy, particularly *z*-filtered TOCSY,[46−50] and dipolar correlated 2D rotating frame nuclear Overhauser enhancement spectroscopy (ROESY).[51,52] The proton spin systems of the individual amino acid residues were identified with the use of a TOCSY spectrum, whereas the sequential resonance assignment relied on the detection of interresidue dipolar interactions between NH-(i+1)/H$^\alpha$(i+1) and H$^\alpha$(i) protons using the 2D ROESY experiment.

^{1}H NMR data, including chemical shifts, coupling constants, and temperature coefficients of amide protons, reported in Table 3 were extracted from the resolution-enhanced 1D spectrum in combination with the highly digitized 1D traces of the *z*-filtered TOCSY spectrum. The assignment of proton resonances was corroborated by proton-detected heteronuclear correlation spectroscopy,[53,54] taking advantage of the large chemical shift dispersion of carbon resonances. The homonuclear coupling constants J(HNC$^\alpha$H) were used to estimate the ϕ angles[55] for the corresponding amino acid residues and to assess the consistency with modeling studies. The J(HC$^\alpha$C$^\beta$H) coupling constants in combination with the observed intraresidue ROE patterns were used for the stereospecific assignments of βH protons and for the determination of preferred side chain conformations.[28−30] ROE cross-peaks were classified according to their intensities as strong (s), medium (m), and weak (w) correlations corresponding to distance constraints of 1.8−2.5, 1.8−3.5, and 1.8−4.5 Å, respectively.[56]

Proton-detected heteronuclear correlation spectroscopy, including multiplet-edited HSQC,[53,54] was used for the assignment of protonated carbon resonances as well as to resolve the ambiguities in the proton resonance assignment. Due to the phase-edited nature of the HSQC spectrum, the origin of the correlations, from either methylene or methine/methyl groups, observed at the respective carbon chemical shift, could easily be determined. The assignment of protonated carbons and the corresponding carbon chemical shift data and one-bond coupling constants (^1J(HC)) are given in Table S1. In addition, the ^{13}C chemical shifts of the D-Pen methyl carbons were used to probe the side chain conformations (dihedral angles χ_1), taking advantage of the well-known conformational dependence of the γ-substituent effect.[31−33] On the basis of simple consideration of γ-effects of the NH and CO functional groups on the chemical shifts of the D-Pen methyls, we could predict the presence of a conformational equilibrium in the case of DPMPT (see the Results). Note that the use of the structurally very sensitive ^{13}C chemical shifts as a conformational probe proved to be invaluable.

Experimental Parameters of NMR Measurements. *Z*-Filtered TOCSY. The *z*-filtered TOCSY spectrum was recorded at 305 K with 4140 Hz spectral width in both dimensions and 4096 complex data points in F2 and 256 data points in F1 with 64 transients at each increment. Quadrature detection in F1 was achieved by TPPI.[57] A relaxation delay of 1.2 s was allowed between successive transients. The isotropic mixing of 60 ms was achieved by the recently introduced TOWNY[50] sequence flanked by two 2.5 ms trim pulses. The TOWNY sequence was designed to suppress the unwanted cross-relaxation peaks in TOCSY experiments. ^{1}H pulses (90° pulse of 27.3 μs) obtained through the decoupler provided a spin-lock field of 9.2 kHz strength. Following the mixing sequence, a randomly varied *z*-filter delay of 15 ms sandwiched between two 90° proton pulses was applied to obtain pure absorption phase data. Zero-filling and multiplication with a squared cosine function in both dimensions were performed prior to 2D Fourier transformation. For evaluation of coupling constants, a

(44) Nyburg, S. C. *Acta Crystallogr*. **1974**, *B30* (part I), 251−253.
(45) Wuthrich, K. *NMR of proteins and nucleic acids*; Wiley-Interscience: New York, 1986.
(46) Braunschweiler, L.; Ernst, R. R. *J. Magn. Reson.* **1983**, *53*, 521−528.
(47) Davis, D. G.; Bax, A. *J. Am. Chem. Soc*. **1985**, *107*, 2820−2821.
(48) Subramanian, S.; Bax, A. *J. Magn. Reson*. **1987**, *71*, 325−330.
(49) Rance, M. *J. Magn. Reson.* **1987**, *74*, 557−564.
(50) Kadkhodaei, M.; Hwang, T. L.; Tang, J.; Shaka, A. J. *J. Magn. Reson., Ser. A* **1993**, *105*, 104−107.
(51) Bothner-By, A. A.; Stephens, R. L.; Lee, J.; Warren, C. D.; Jeanloz, R. W. *J. Am. Chem. Soc*. **1984**, *106*, 811−813.
(52) Bax, A.; Davis, D. G. *J. Magn. Reson*. **1985**, *63*, 207−213.
(53) Davis, D. G. *J. Magn. Reson*. **1991**, *91*, 665−672.
(54) Kövér, K. E.; Prakash, O.; Hruby, V. J. *J. Magn. Reson. Chem.* **1993**, *31*, 231−237.
(55) Bystrov, V. F. *Prog. Nucl. Magn. Reson. Spectrosc*. **1976**, *10*, 41−81.
(56) Bax, A. *Annu. Rev. Biochem*. **1989**, *58*, 223−256.
(57) Marion, D.; Wuthrich, K. *Biochem. Biophys. Res. Commun*. **1983**, *113*, 967−974.

final digital resolution of 0.3 Hz/point was achieved by inverse Fourier transformation, zero-filling, and back-transformation of selected traces.

ROESY. ROESY experiments were performed at 305 K using 200 ms of CW spin-lock field in inverse mode. The ^{1}H 90° pulse of 75 μs was obtained through the decoupler. A relaxation delay of 1.2 s was allowed between successive scans. A total of 160 scans were recorded with 2K complex data points each for a total number of 256 experiments. For data processing the matrices were zero-filled and apodized by a squared cosine function in both dimensions. Since the NH signals of DPMPT were broad at 305 K, a ROESY spectrum at 325 K was also recorded. At this elevated temperature the NH signals became considerably sharper, allowing the detection of several additional important ROE contacts.

Multiplet-Edited HSOC. In the ^{1}H/^{13}C correlation experiments the spectral parameters and pulse durations were used as follows: 4140 Hz for ^{1}H; 13 080 Hz for ^{13}C; ^{1}H 90° pulse, 7.3 μs; ^{13}C 90° pulse, 12.0 μs; spin-lock pulses of 1.5 ms were applied for suppression of ^{1}H−^{12}C magnetization. A total of 64 scans were acquired with 2K complex data points for 200 t_1 increments. A relaxation delay of 0.8 s was allowed between successive transients. The INEPT delay was set to 1.8 ms. Data matrices were zero-filled and apodized with the cosine square function in both dimensions.

X-ray Analysis. A stock solution of DPDMPT was prepared by dissolving 3.4 mg of the peptide in 0.25 mL of 50% EtOH. Several crystallization experiments (using both hanging and sitting drops) were then set up using various buffers and varying concentrations of PEG and MPD. The crystals used for data collection grew in a 10 μL sitting drop containing a 1:1 mixture of stock solution and the aqueous well solution (35% ETOH and 10% MPD). The data crystal was transferred from the sitting drop into high-viscosity microscope oil. It was then mounted on a glass rod and transferred immediately to the cold stream (−60 °C) of an automatic 4-circle Siemens R3m/V diffractometer for data collection. The cell dimensions, given in Table 9 together with other relevant crystal data, were determined from a least-squares refinement of the angular positions for 25 reflections with 2θ values ranging from 50.3° to 60.1°. The diffractometer, equipped with a graphite monochromator, was used in the $\theta/2\theta$ scan mode with a variable 2θ scan speed ranging from 4 to 15 deg/min, depending upon the intensity of a reflection, to collect data out to $2\theta_{max}$ of 112°. Three standard reflections repeated after every 97 reflections showed a random variance of ±2.5%, indicating that the crystal did not deteriorate during data collection. The data were corrected for Lorentz and polarization effects, and a face-indexed absorption correction was applied (minimum and maximum transmission factors were 0.613 and 0.870, respectively).

The DPDMPT structure was solved by direct methods using the program SHELXTL.[58] The asymmetric unit contains one peptide molecule and two molecules of ethanol. The structure was refined using a full-matrix least-squares method on F^2 values using the program SHELXL93[59] on the full set of 2589 independent reflections. Coordinates and anisotropic thermal parameters were refined for all nonhydrogen atoms. Hydrogen atoms were placed at calculated positions and were allowed to ride on their covalently bonded atoms (C−H = 0.98 Å, N−H = 0.86−0.89 Å, and O−H = 0.82−0.85 Å). Isotropic hydrogen thermal parameters were reset at the end of each refinement cycle to be equal to $1.1U_{eq}$ of their covalently bonded atoms, $1.2U_{eq}$ for methyl hydrogens, and $1.3U_{eq}$ for hydroxyl hydrogens on the ethanol molecules. The final R factors are given in Table 9. Atomic coordinates for all atoms are available from the Cambridge Crystallographic Data Centre, Cambridge University Chemical Laboratory, Cambridge CB2 1EW, U.K., and through the LSM Home Page under the heading neuropeptide structure (URL http://lsm-www.nrl.navy.mil/doc/neuro-pep/html).

Opioid Receptor Binding Assays. Affinity for opioid receptors was determined in Tris−HCl buffer, pH 7.4, using the standard *in vitro* competition assay procedures previously described in detail.[60,61] A crude membrane preparation from guinea pig brain was used. Opioid receptor subtypes were labeled using 1.25 nM [^{3}H]DPDPE ± 1 μM [D-Ala^2,D-Leu^5]-enkephalin (δ), 0.15 nM [^{3}H]DAMGO ± 1 μM naloxone (μ), and 1.25 nM [^{3}H]U-69,593 ± 1 μM ethylketocyclazocine (κ_1). Bound and free [^{3}H]ligands were separated by filtration through Schleicher and Schuell no. 32 glass fiber filters. Inhibition constants were calculated using the computer program *Equilibrium Binding Data Analysis* (Elsevier-BIOSOFT) and gave K_d values of 1.74, 0.5, and 1.34 nM for δ-, μ-, and κ_1-receptors, respectively.

Acknowledgment. This study was supported in part by Grants GM-24483 and GM-48184 from the NIH. S.A.K. was a recipient of a Postdoctoral Training Grant in Neuropharmacology (T32 NS07129) from the NIH. B.N. is recipient of the Research Scientist Development Award DA-00157 from NIDA. K.E.K. acknowledges support from the Hungarian Academy of Sciences (Grant OTKA T-014982) and the assistance of Peter Forgo in the NMR measurements. We also acknowledge the support of NIDA and the Office of Naval Research in the X-ray studies.

Supporting Information Available: Text describing the syntheses of **1**, **2a**, and **2b** and the geometrical comparison of conformers, tables giving ^{13}C NMR data for DPDMPT and DPMPT and hydrogen bond parameters, atomic coordinates, isotropic and anisotropic displacement parameters, and bond lengths and angles for DPDMPT, and a figure showing a fragment of the 2D TOCSY spectrum for DPDMPT (11 pages). This material is contained in many libraries on microfiche, immediately follows this article in the microfilm version of the journal, can be ordered from the ACS, and can be downloaded from the Internet; see any current masthead page for ordering information and Internet access instructions.

JA952964+

(58) Sheldrick, G. M. *SHELXTL-Plus. Release 4.2*; Siemens Analytical X-ray Instruments: Madison, WI, 1993.

(59) Sheldrick, G. M.; Scheider, T. R. *Methods Enzymol*., submitted for publication.

(60) Nock, B.; Giordano, A. L.; Cicero, T. J.; O'Connor, L. H. *J. Pharmacol. Exp. Ther*. **1990**, *254*, 412−419.

(61) Nock, B.; Giordano, A. L.; Moore, B. W.; Cicero, T. J. *J. Pharmacol. Exp. Ther*. **1993**, *264*, 349−359.